nature genetics

Mutations in amphiphysin 2 (*BIN1*) disrupt interaction with dynamin 2 and cause autosomal recessive centronuclear myopathy

Anne-Sophie Nicot[1,7], Anne Toussaint[1,7], Valérie Tosch[1], Christine Kretz[1], Carina Wallgren-Pettersson[2], Erik Iwarsson[3], Helen Kingston[4], Jean-Marie Garnier[1], Valérie Biancalana[5], Anders Oldfors[6], Jean-Louis Mandel[1,5] & Jocelyn Laporte[1]

Centronuclear myopathies are characterized by muscle weakness and abnormal centralization of nuclei in muscle fibers not secondary to regeneration. The severe neonatal X-linked form (myotubular myopathy) is due to mutations in the phosphoinositide phosphatase myotubularin (*MTM1*)[1], whereas mutations in dynamin 2 (*DNM2*) have been found in some autosomal dominant cases[2]. By direct sequencing of functional candidate genes, we identified homozygous mutations in amphiphysin 2 (*BIN1*) in three families with autosomal recessive inheritance. Two missense mutations affecting the BAR (Bin1/amphiphysin/RVS167) domain disrupt its membrane tubulation properties in transfected cells, and a partial truncation of the C-terminal SH3 domain abrogates the interaction with DNM2 and its recruitment to the membrane tubules. Our results suggest that mutations in *BIN1* cause centronuclear myopathy by interfering with remodeling of T tubules and/or endocytic membranes, and that the functional interaction between BIN1 and DNM2 is necessary for normal muscle function and positioning of nuclei.

Centronuclear myopathies (CNMs) have been divided into three forms: the X-linked form (OMIM 310400) with severe hypotonia at birth; autosomal recessive forms with onset of weakness in infancy or early childhood with or without ophthalmoparesis (OMIM 255200); and a dominant form that usually appears in adulthood and is slowly progressive (OMIM 160150)[3–5]. Myotubularin dephosphorylates a subclass of phosphoinositides important for endocytosis and is probably involved in membrane trafficking[6,7], suggesting that CNMs arise from membrane trafficking defects. Identification of mutations in the gene encoding dynamin 2 in individuals with the dominant form has supported this hypothesis, as dynamin 2 is a large GTPase with important roles in endocytosis, membrane trafficking, actin assembly and centrosome function[2,8]. In a sporadic CNM case with childhood onset, we have reported an inactivating variant affecting a

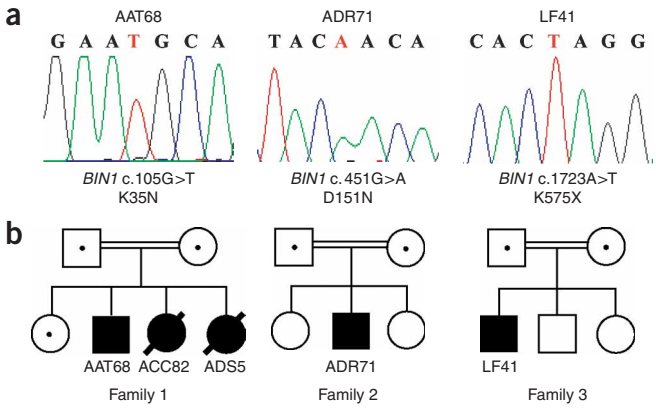

Figure 1 *BIN1* mutations in patients with recessive centronuclear myopathy. (**a**) Chromatograms from index cases. Homozygous mutations are in red, numbered based on the reference sequence of BIN1 isoform 1 (593 amino acid residues in length). These mutations lead to two amino acid changes (K35N and D151N) and one premature stop codon (K575X). (**b**) Pedigrees of consanguineous families 1–3 (with first-cousin consanguineous parents). Dots indicate heterozygous carriers; filled squares and circles, affected individuals. Except for ADS5 (for whom DNA was not available), all affected individuals are homozygous for the variants. The healthy sister of AAT68 is heterozygous for the K35N variant, and the healthy sisters of ADR71 do not carry the D151N variant; DNA was not available for the healthy brother and sister of LF41.

[1]Institut de Génétique et de Biologie Moléculaire et Cellulaire (IGBMC), Department of Molecular Pathology, F-67400 Illkirch, France; Institut National de la Santé et de la Recherche Médicale (INSERM), U596, F-67400 Illkirch, France; the Centre National de la Recherche Scientifique (CNRS), UMR7104, F-67400 Illkirch, France; Université Louis Pasteur, F-67000 Strasbourg, France; and Collège de France, Chaire de Génétique Humaine, F-67400 Illkirch, France. [2]Department of Medical Genetics, University of Helsinki, and The Folkhälsan Institute of Genetics, Biomedicum, FIN-00014 Helsinki, Finland. [3]Clinical Genetics Unit, Department of Molecular Medicine and Surgery, Karolinska University Hospital, S-171 76 Stockholm, Sweden. [4]Academic Unit of Medical Genetics and Regional Genetic Service, Central Manchester and Manchester Children's University Hospitals, Manchester M13 OJH, UK. [5]Laboratoire de Diagnostic Génétique, CHRU–Faculté de Médecine et Laboratoire de Génétique Médicale EA3949, Université Louis Pasteur, Strasbourg F-67085, France. [6]Department of Pathology, Sahlgrenska University Hospital, SE-413 45 Göteborg, Sweden. [7]These authors contributed equally to this work. Correspondence should be addressed to J.L. (mtm@igbmc.u-strasbg.fr).

Received 23 December 2006; accepted 31 May 2007; published online 5 August 2007; doi:10.1038/ng2086

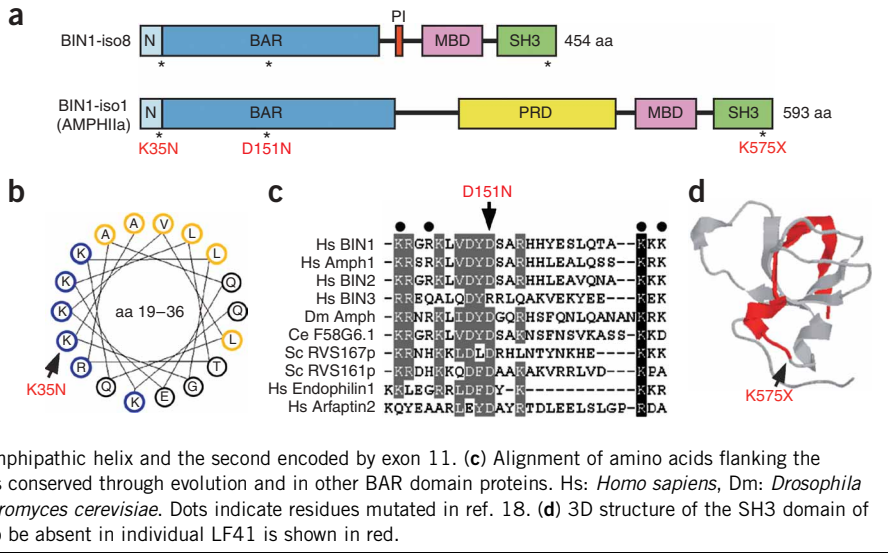

Figure 2 Localization of amino acid changes in BIN1. (**a**) Protein domains of BIN1 isoforms. N, N-terminal amphipathic helix; BAR, BIN1/Amphiphysin/Rvs167; PI, phospoinositide-binding domain, corresponding to a polybasic residue sequence encoded by exon 11; PRD, proline-rich domain binding to clathrin and AP-2; MBD, Myc-binding domain; SH3, Src homology 3. The muscle-specific BIN1 isoform 8 lacks the PRD present in the brain-enriched BIN1-iso1 (AMPHIIa) and contains an additional PI domain. Positions of the residues affected by mutations are indicated with asterisks. (**b**) Helical wheel projection of amino acid (aa) residues 19–36 of BIN1 showing the presence of an amphipathic helix and a stretch of polybasic residues (nonpolar residues in orange, basic residues in blue). There are thus two stretches of polybasic residues, one located on one side of the N-terminal amphipathic helix and the second encoded by exon 11. (**c**) Alignment of amino acids flanking the D151N missense change, showing that this position is conserved through evolution and in other BAR domain proteins. Hs: *Homo sapiens*, Dm: *Drosophila melanogaster*, Ce: *Caenorhabditis elegans*, Sc: *Saccharomyces cerevisiae*. Dots indicate residues mutated in ref. 18. (**d**) 3D structure of the SH3 domain of rat Bin1. The corresponding region that is predicted to be absent in individual LF41 is shown in red.

new phosphoinositide phosphatase, hJUMPY, which shares the same substrate specificity as myotubularin[9].

Thus far, the gene(s) implicated in recessive CNM have not been identified or even localized. As the lack of large families precluded positional cloning, we directly sequenced functional candidate genes in a panel of individuals with CNM, based on the assumption that implicated proteins have cellular functions related to myotubularin. BIN1 seemed to be a good candidate, as it is involved in membrane remodeling, is regulated by phosphoinositides[10] and has a role in the organization of T tubules[11], which are thought to be altered in X-linked myotubular myopathy (XLMTM)[12]; in addition, defects of the *Drosophila melanogaster* ortholog lead to skeletal muscle alterations[13]. The *BIN1* gene encompasses 20 exons, some of which are alternatively spliced, leading to at least ten different isoforms[14–16]. We refer to the largest isoform, AMPHIIa, as BIN1-iso1, and to the muscle-specific M-amphiphysin isoform as BIN1-iso8.

Our collection of individuals with CNM includes families with probable recessive inheritance (offspring of consanguineous parents), sporadic cases and severe cases initially thought to have XLMTM but lacking *MTM1* mutations (**Supplementary Note** online). All showed centralization of nuclei in muscle fibers. Direct sequencing of *BIN1* in samples from 55 affected individuals showed three homozygous variants in four affected individuals from three consanguineous families (**Fig. 1**; see also **Supplementary Tables 1** and **2** online for primer sequences and the observed polymorphisms). The three variants, which include two amino acid changes (K35N and D151N) and a premature stop codon (K575X), were present in the homozygous state in all affected individuals tested within these families, whereas parents were heterozygous, and unaffected relatives were heterozygous or did not carry the variants (**Fig. 1**). These variants were absent in at least 280 genomic DNA samples from unaffected controls, including controls of the same geographic origin, and we confirmed that *MTM1* and *DNM2* were not mutated in these families by direct sequencing of exons and intron-exon boundaries. By whole-genome SNP analysis using DNA microarrays, we confirmed that affected individuals AAT68 and ADR71 were homozygous for the chromosomal region 2q14, where *BIN1* is located (**Supplementary Fig. 1** online). Affected individual LF41 did not show a large

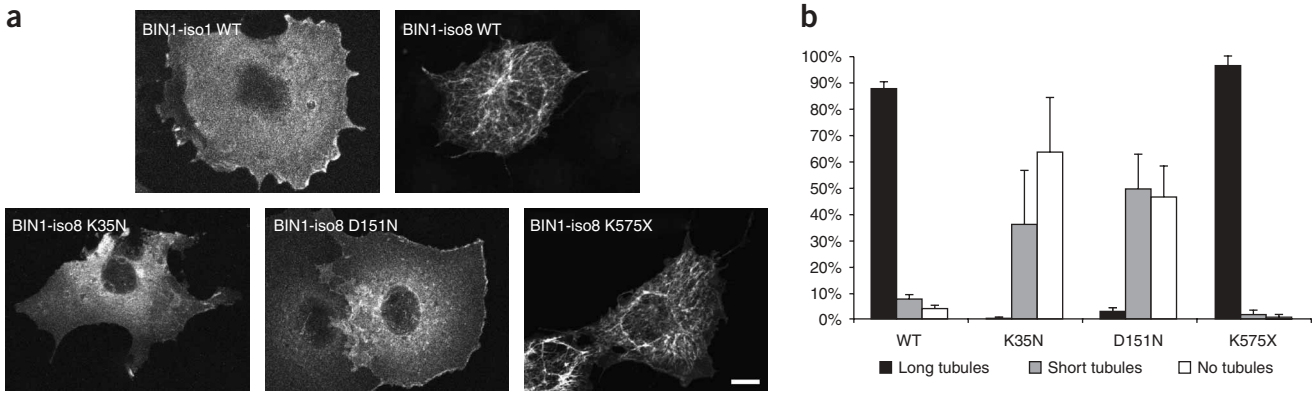

Figure 3 *Ex vivo* membrane tubulation assays. COS-1 cells were transfected with cDNA constructs encoding BIN1-iso1, wild-type (WT) BIN1-iso8 or mutant BIN1-iso8. Overexpressed BIN1-iso1 was detected with C99D, and BIN1-iso8 constructs were fused to GFP. Constructs encoding wild-type BIN1-iso8 and BIN1-iso8 with the K575X change induce membrane tubulation, contrary to BIN1-iso1 and BAR domain mutants. (**a**) Representative images from confocal projections. Scale bar: 10 μm. (**b**) Quantification of three independent experiments. For each construct, we show the percentage of cells with long tubules (as in BIN1-iso8 wild-type in **a**), short tubules (with lengths of no more than about four times their width) or no tubules at all. At least 100 cells were assessed per experiment. Error bars indicate s.e.m.

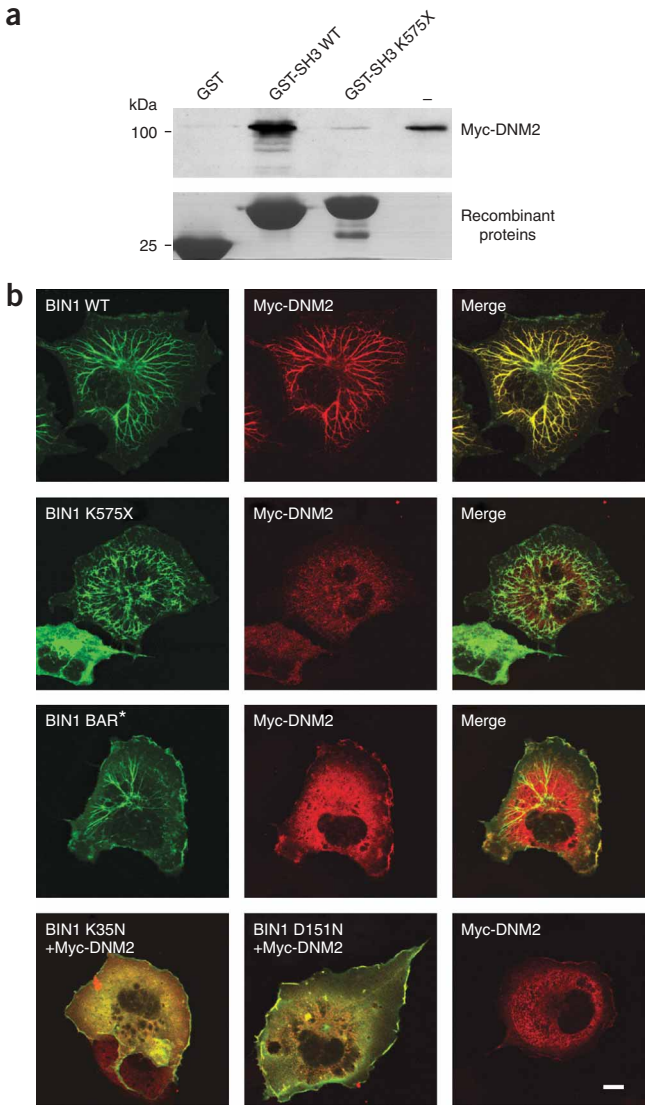

Figure 4 Dynamin 2–BIN1 interaction and recruitment to membrane tubules. (**a**) Interaction of dynamin 2 (DNM2) with the BIN1 SH3 domain. GST-tagged recombinant BIN1 SH3 domain proteins were used to pull down Myc-tagged dynamin 2 overexpressed in COS-1 cells. Lane marked "–" shows the crude cell extract before pull-down. Upper panel: protein blot hybridized with anti-Myc; lower panel: Coomassie staining of the recombinant proteins from the same acrylamide gel. The deleted GST-SH3 K575X recombinant protein migrates higher than the wild-type protein; their integrity was confirmed by peptide mass fingerprinting. Representative images of three different experiments are shown. (**b**) Dynamin 2 recruitment to BIN1-iso8–induced membrane tubules. COS-1 cells were transfected with Myc-tagged dynamin 2 and different GFP-tagged BIN1 constructs: wild-type and mutated full length BIN1-iso8 and wild-type BAR* (amino acids 1–282, containing the phosphoinositide binding domain of exon 11 but lacking the SH3 domain). Dynamin 2 localization was detected with anti-Myc. Dynamin 2 recruitment to the membrane tubules induced by BIN1-iso8 was dependent on a wild-type SH3 domain. The bottom panel shows merged images of cells expressing DNM2 together with BAR domain mutants or dynamin 2 alone. Confocal single scan images are representative of several experiments. Scale bar, 10 μm.

homozygous region at 2q14, although he has a homozygous mutation in *BIN1*, and we did not find a *BIN1* variant in the unrelated consanguineous affected individual ABJ25, who showed homozygosity not only at 2q14 but also at other chromosome regions. Our data also point to the heterogeneity of recessive CNM, as we found mutations in only 3 out of 12 families with some documentation of recessive inheritance.

All affected individuals with mutations had the typical CNM muscle histology, showing numerous fibers with central nuclei (data not shown). Onset of the disease ranged from birth to childhood; three out of five affected individuals are still alive, showing mild, proximal, slowly progressive muscle weakness, and unlike in the X-linked severe form of the disease, assisted ventilation was not needed (**Supplementary Table 3** online). The phenotype of these individuals is thus intermediate between the X-linked and dominant forms; individual LF41, carrying the K575X change leading to a premature stop codon, seems to be the most severely affected. Affected individuals from family 1 showed mild to severe congenital contractures. Apart from underdevelopment of both frontal lobes in ACC82, possibly linked to intrauterine growth retardation, we did not observe any effects in other tissues besides muscle, and there was no cognitive impairment.

BIN1 protein domains are implicated in membrane tubulation and in protein-lipid and protein-protein interactions (**Fig. 2**). An N-terminal amphipathic helix is believed to insert into the plasma membrane and create curvature, and the BAR domain homodimerizes to form a banana shape that is able to sense and maintain the curvature[17,18]. The C-terminal SH3 domain mediates interactions with numerous proteins such as synaptojanin and dynamin. All isoforms have the BAR and SH3 domains and also a Myc-binding domain[19,20]. In addition, the neuronal isoforms have a clathrin- and AP-2-binding domain, and the so-called muscle-specific BIN1-iso8 has a polybasic residue sequence binding to phosphoinositides, located C-terminal of the BAR domain[10,11].

Helical wheel projection of amino acid residues 19–36 suggested the presence of an amphipathic helix together with a stretch of polybasic residues. The latter may represent a new domain of interaction with negatively charged lipids N-terminal of the BAR domain (**Fig. 2**). The K35N missense change is predicted to alter the charge of this polybasic sequence, suggesting that it may lead to a defect in membrane curvature. The D151N missense change alters a residue conserved through evolution down to the yeast amphiphysin-like proteins, and in other BAR domains, and replacement of the four flanking residues has been shown to strongly reduce liposome tubulation[18]. Finally, we predicted that the K575X change removes the last alpha-helix and two beta-strands of the SH3 domain, a region highly conserved through evolution and implicated in the three-dimensional (3D) structure of the domain[21]. A missense mutation affecting a phenylalanine residue in this region, corresponding to F588, was sufficient to decrease the binding to dynamin[21].

To test the impact of the mutations found in individuals with CNM, we monitored the membrane tubulation properties of wild-type and mutated BIN1 in cells and assessed binding to dynamin 2. As already described, overexpressed BIN1-iso8 was capable of tubulating membranes *ex vivo* (**Fig. 3** and ref. 11). Introduction of the missense mutations found in families 1 and 2 abolished membrane tubulation (**Fig. 3**). As expected, the K575X change did not affect membrane tubulation. Dynamin 1 is well known to interact with the SH3 domain of amphiphysin 1 in the brain, and dynamin 2 also interacts with BIN1 (ref. 10). The SH3 domain of BIN1 was able to pull down dynamin 2 overexpressed in COS cells, and introduction of the premature stop codon K575X found in family 3 clearly weakened the binding (**Fig. 4a**). Taken together, these data show that mutations found in individuals with CNM have a strong impact on various functions of BIN1.

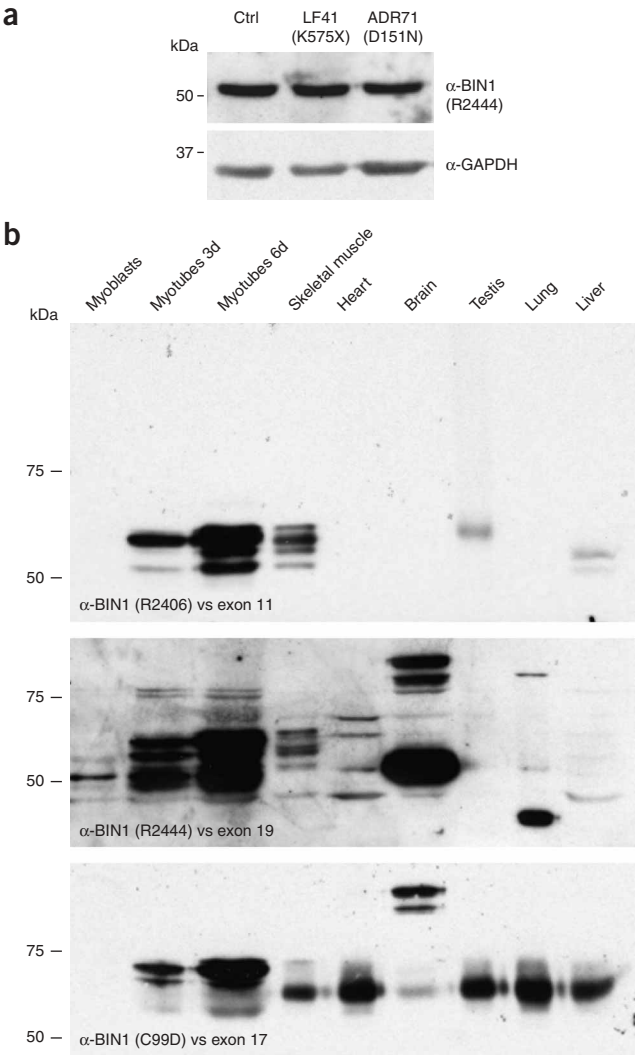

Figure 5 BIN1 expression in normal and pathological conditions. (**a**) BIN1 protein expression in fibroblast cell lines from individuals LF41 and ADR71 and from a control. No cells were available for the K35N change. BIN1 was detected with antibody R2444 directed against the n-Src loop of the SH3 domain, and GAPDH was used as an internal loading control. (**b**) Mouse Bin1 expression and isoforms in mouse C2C12 muscle cells during differentiation (myoblasts, 3 d and 6 d after the start of differentiation into myotubes) and in mouse tissues. Bin1 was detected with antibody R2406 directed against exon 11, antibody R2444 against exon 19 and antibody C99D against exon 17. Equal loading was monitored by Ponceau red and Coomassie staining. Note the presence of at least four isoforms encompassing the polybasic residue sequence of exon 11 in skeletal muscle.

Notably, dynamin 2 mutations cause dominant CNM[2], and our present work implicates mutations in *BIN1* in recessive CNM. Thus, we tested the recruitment of dynamin 2 to the membrane tubules induced by overexpression of BIN1-iso8. With wild-type constructs, we noted a marked recruitment of dynamin 2 (**Fig. 4b** and ref. 11). This recruitment was dependent on the SH3 domain, as the construct BIN BAR* lacking this domain was able to tubulate membranes but did not recruit dynamin 2. Whereas K35N and D151N did not induce tubulation, the K575X mutant induced membrane tubulation but was not able to efficiently recruit dynamin 2 to these tubules (**Fig. 4b**). Our results suggest that mutations in *BIN1* found in individuals with CNM cause a loss of the functional link with dynamin 2.

Loss of BIN1 expression is a common feature in malignant cells. In particular, *BIN1* is widely downregulated or misspliced in cancers of the breast, prostate, colon, brain and other organs[20,22–24]. Moreover, *Bin1* knockout mice show perinatal death associated with cardiomyopathy[25]. However, neither cardiac dysfunction nor cancer history were noted in the three individuals with CNM still alive. The selective and highly specific skeletal muscle phenotype that is observed in the three families with *BIN1* mutations contrasts with these previously published data. We propose that this observation is due to a combination of two factors: (i) the mutations elicit only a partial loss of function, and (ii) BIN1 has an important role in skeletal muscle that may be sensitive to mutations whose effects can be compensated for in other tissues. Indeed, we have observed that the D151N and K575X changes do not have a detectable impact on the expression of BIN1 protein in affected individuals' fibroblasts (**Fig. 5a**). The nonsense K575X change occurs in the last exon of the gene; this does not lead to nonsense-mediated mRNA decay and truncates only the 19 most C-terminal amino acid residues. Second, expression analysis of Bin1 in mouse tissues with three different antibodies showed that its expression and the number of isoforms present increased with muscle cell differentiation (from myoblasts to myotubes), supporting an important role for

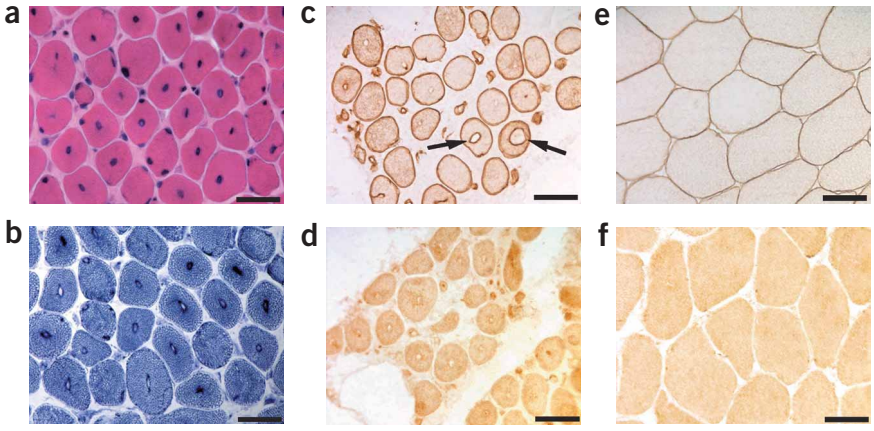

Figure 6 Biopsy from the deltoid muscle of individual ADR71. (**a**) Centrally located nuclei are present in virtually every fiber (see by hematoxylin-eosin staining). (**b**) NADH-tetrazolium reductase staining, demonstrating that centrally located nuclei are surrounded by a rim of densely stained material. Radial organization of the sarcoplasmic reticulum, a hallmark of dominant CNM with *DNM2* mutations, was not present. (**c**) Immunostaining of caveolin 3, showing positive immunoreactivity associated with centrally located vacuoles in some fibers (arrows). Numerous fibers showed increased caveolin 3 immunoreactivity associated with the intermyofibrillar network. (**d**) Immunostaining of the T tubule marker dihydropyridine receptor-α (DHPRα), demonstrating marked immunoreactivity around centrally located nuclei. (**e**,**f**) Caveolin 3 (**e**) and DHPRα immunoreactivity (**f**) in control muscle. Scale bar, 20 μm.

it in skeletal muscle, consistent with previous studies (**Fig. 5b** and refs. 11,14,26). We detected at least four muscle isoforms containing exon 11; only isoform 8 had been previously characterized, suggesting the existence of additional muscle-specific isoforms (**Fig. 5b**).

A few studies have reported that BIN1 is implicated in the organization of T tubules[11,13], a specialized membrane structure involved in excitation-contraction coupling[27]. Immunostaining of a muscle biopsy from individual ADR71 (with the D151N change) using markers associated with T tubules during development or in mature muscle showed increased caveolin 3 and DHPRα labeling inside the fibers and abnormal caveolin 3–positive vacuoles (**Fig. 6**). We hypothesize that perturbation of T tubule biogenesis and/or endocytic membranes by mutations in *BIN1* could be the primary cause of the muscle pathology in CNM. The most obvious pathological feature in CNM is the central location of nuclei. This does not seem to be related to a previously hypothesized defect in muscle maturation, because in the mouse model for XLMTM, the skeletal muscle fibers have subsarcolemmal nuclei at birth, whereas CNM pathology appears later[28]; however, this has not yet been confirmed in humans with CNM. Either nucleus centralization is a secondary consequence of abnormalities in membrane remodeling, or myotubularin, dynamin 2 and BIN1 have an independent role in the maintenance of skeletal muscle fiber organization and, in particular, positioning of nuclei.

METHODS

Mutation screening and haplotype analysis. Exonic coding sequence and exon-intron boundaries for *BIN1*, *MTM1* and *DNM2* were sequenced after PCR amplification of genomic DNA using intronic primers[1,2] (**Supplementary Table 1** online for *BIN1*). We observed segregation of the mutations in family members by direct sequencing of exons 2, 6 or 20. We checked for the absence of the variants in control DNA from nonmyopathic individuals by denaturing HPLC (exons 2 and 20) or by direct sequencing (exon 6). PCR products were purified using Multiscreen HTS 96-wells plates (Millipore) and were analyzed with an ABI PRISM BigDye Terminator cycle using a 3130XL genetic analyzer (Applied Bioscience). For whole-genome haplotype analysis, subjects' genomic DNA was hybridized to Affymetrix 10K SNP arrays according to the manufacturer's instructions, and loss of heterozygosity was analyzed with GeneChip DNA Analysis and Chromosome Copy Number Analysis software (Affymetrix).

Amino acid sequence analysis. We used CLUSTAL_X[29] for amino acid alignment of the following proteins: human BIN1, AMPH1, BIN2, BIN3, *Drosophila melanogaster* amphiphysin, *Caenorhabditis elegans* amphiphysin, *Saccharomyces cerevisiae* RVS167p and RVS161p and human endophilin 1 and arfaptin 2.

cDNA constructs. cDNAs corresponding to BIN1-iso8 (454 amino acid residues long), BIN1 BAR* (residues 1–282) and BIN1 SH3 domain (residues 497–593) were gifts (see Acknowledgments), and cDNA corresponding to BIN1-iso1 (AMPHIIa, 593 residues long) was obtained from the Deutsches Ressourcenzentrum für Genomforschung (clone DKFZp547F068Q). The dynamin 2 cDNA, obtained from Geneservice (IMAGE clone 5722134), was cloned into a pENTR1A Gateway entry vector (Invitrogen) and recombined into the pTL1 destination vector, a derivative of the pSG5 vector[30], for C-terminal Myc-His tag fusion. Mutations were introduced by primer-directed PCR mutagenesis, and all constructs were verified by sequencing. For GST pull-down, cDNAs cloned into the pGEX-2T vector (GE Healthcare) were used to produce the relevant proteins with N-terminal GST tags. For eukaryotic cell transfection, BIN1-iso8 cDNA was cloned into pEGFP-C1 (Clontech) and overexpressed as an N-terminally EGFP-tagged protein, and BIN1-iso1 was cloned into pCDNA3.1 (Invitrogen) and overexpressed without any protein tag.

Expression analysis. Two rabbit antibodies were generated: R2406 antibodies raised against a peptide corresponding to exon 11 of BIN1 (RKKSKLFSRLRRKKN) and R2444 antibodies raised against the n-src loop of the SH3 domain in exon 19 (peptide VIPFQNPEEQDEG). Sera were purified on peptide-coupled SulfoLink columns (Pierce) and were validated on COS-1 cells transfected with BIN1 isoforms and using peptide competition. Mouse monoclonal antibody C99D (Upstate) is directed against the Myc-binding domain in exon 17.

After obtaining informed consent from participants, and using procedures approved by the Regional Ethical Review Board in Gothenburg and the North Manchester Research Ethics Committee, we cultured control and CNM fibroblasts from their skin biopsies in DMEM containing 1g/l glucose, supplemented with 10% FCS and 40 mg/l gentamicin (37 °C, 5% CO_2). Proteins were extracted with TGEK50 buffer (50 mM Tris (pH 7.8), 10% glycerol, 1 mM EDTA, 50 mM KCl) with 0.1% SDS, 2% Triton and a cocktail of protease inhibitors (PIC) containing 2.5 µg/ml of each of the following: leupeptin (Euromedex), pepstatin A (Euromedex), aprotinin (Euromedex), antipain (Chemicon) and chymostatin (Sigma). We boiled 30 µg of each protein in loading buffer (8% SDS, 0.4 M DTT, 240 mM Tris pH 6.8, 0.004% bromophenol blue, 40% glycerol) and subjected them to electrophoresis on an 8% SDS-polyacrylamide gel. Proteins were transferred onto nitrocellulose membranes that were blocked with 3% BSA in PBS with 0.1% Tween-20 and incubated with R2444 antibody for 2 h. For detection, we used secondary antibody coupled with HRP with Supersignal Substrate (Pierce), followed by autoradiography.

Total proteins were extracted from skeletal muscle, heart, brain, testis, lung and liver of adult mice and from C2C12 cells at several differentiation stages. Undifferentiated C2C12 cells were cultured in DMEM containing 1g/l glucose supplemented with 20% FCS and 40 mg/l gentamicin. Differentiation of myoblasts into myotubes was induced at 80% confluence by addition of DMEM containing 1g/l glucose supplemented with 5% horse serum (HS) and 40 mg/l gentamicin. Cells or tissues were incubated for 5 min on ice in 10 mM $NaHCO_3$ and 2 mM $CaCl_2$ supplemented with PIC. Cells were scraped and tissues crushed in an Ultra Thurax homogenizer, and an equal volume of a second solution (500 mM sucrose, 300 mM KCl, 4 mM $MgCl_2$, 60 mM histidine, pH 7.4) was added. After centrifugation (500*g*, 20 min, 4 °C), the total protein extracts were separated on a 10% SDS-polyacrylamide gel and were transferred onto nitrocellulose membranes that were blocked with 5% nonfat dry milk in TBS-T buffer (TBS plus 0.1% Tween-20). Membranes were incubated with primary antibodies for 1 h for the polyclonal antibody to BIN1 (R2406; 1:10,000) or 2 h for the polyclonal antibody to BIN1 (R2444; 1:400) and for the monoclonal antibody to BIN1 (C99D from Upstate; 1:200) in TBS-T buffer containing 5% nonfat dry milk. Secondary antibodies (anti-rabbit horseradish peroxidase (HRP) or anti-mouse HRP, Jackson ImmunoResearch) were incubated for 1 h.

Pull-down assays. Whole-cell extracts from COS-1 cells transfected with Myc-DNM2 were obtained by lysis with a buffer containing 20 mM HEPES-NaOH pH 7.4, 300 mM NaCl, 0.1% Triton X-100, 10% glycerol, 4 mM DTT, 1 mM EDTA, 1 mM sodium orthovanadate and PIC. Extracts were passed through a 25G needle five times to disperse aggregates, and insoluble material was removed by centrifugation at 10,000*g* for 10 min. GST fusion proteins were expressed in *Escherichia coli* strain CodonPlus BL21. Bacteria were lysed by sonication in lysis buffer (PBS with 2 mM EDTA and PIC) and then centrifuged at 10,000*g* for 10 min. GST fusion proteins were purified from bacterial lysates by incubation with glutathione Sepharose 4B beads (GE Healthcare) in lysis buffer with 1% Triton for 2 h followed by extensive washing with PBS plus 1 mM EDTA, 300 mM NaCl, 1 mM DTT, 0.1% Tween-20 and PIC (pH 7.3). We then incubated 2.5 mg of the purified fusion proteins coupled to glutathione beads for 6 h with transfected COS-1 cell extracts (prepared as described above). After washing beads three times with a buffer containing 20 mM HEPES, 400 mM NaCl, and 1 mM DTT (pH 7.3), we analyzed 5 µl of the beads (300 µg of GST-fused proteins bounded to the beads) by electrophoresis on an 8% SDS-polyacrylamide gel. Bound dynamin 2 was detected by a monoclonal antibody to Myc, 9E10 (1:1,000; IGBMC). The entire procedure was carried out at 4 °C.

***Ex vivo* tubulation and subcellular localization.** COS-1 cells were grown in DMEM containing 1g/l glucose supplemented with 5% FCS and 40 mg/l

gentamicin. Cells were grown on 22-mm^2 cover slips and were transfected at 80% confluence with 1 μg of DNA constructs using the Fugene-6 reagent, following the manufacturer's instructions (Roche). Cells were fixed with 4% paraformaldehyde for 20 min and then washed in PBS. For immunolabeling, cells were subsequently permeabilized in PBS with 0.2% Triton X-100 and washed with PBS. Nonspecific sites were blocked in PBS with 10% FCS and 0.1% Triton X-100.

The subcellular localization of proteins was assessed by incubation for 1 h with monoclonal antibodies diluted in PBS with 3% FCS and 0.1% Triton X-100. BIN1-iso1 was detected with an antibody to BIN1 (C99D, Upstate) diluted at 1:200; Myc-DNM2 was detected with an antibody to Myc (9E10; IGBMC) diluted at 1:400. After washing with PBS with 0.1% Triton X-100, we detected immunostaining by incubation for 45 min with a Cy3 mouse secondary antibody. Fluorescence was examined with a Leica SP2-AOBS confocal microscope. Pictures were processed with Tcstk software (Jean-Luc Vonesch, IGBMC) and edited using Dvrtk software (Jean-Luc Vonesch, IGBMC) and Photoshop 7.0 (Adobe).

Immunohistochemistry. Cryostat sections of fresh frozen skeletal muscle (8 μm thick) were incubated with an antibody to caveolin 3 (A-3) (Santa Cruz Biotechnology) diluted 1:1,000 in 1% BSA or with antibody to dihydropyridine receptor-α (DHPRα) (Abcam) diluted 1:3,000 in 1% BSA. Immunoreactivity was visualized by Novolink Polymer Detection System (Novocastra).

Accession numbers. GenBank: *BIN1* isoform 1 mRNA, NM_139343; BIN1 isoform 1 protein, NP_647593; *BIN1* isoform 8 mRNA, NM_004305; BIN1 isoform 8 protein, NP_004296; human BIN1, O00499; amphiphysin 1, P49418; BIN2, Q9UBW5; BIN3, Q9NQY0; *Drosophila melanogaster* amphiphysin, Q7KLE5; *Caenorhabditis elegans* amphiphysin, Q21004; *Saccharomyces cerevisiae* RVS167p, P39743; *S. cerevisiae* RVS161p, P25343; human endophilin 1, Q99962; human arfaptin 2, P53365. Protein Data Bank: three-dimensional structure of the rat Bin1 SH3 domain, 1BB9.

URLs. Helical wheel projection was performed online at http://kael.net/helical.htm.

Note: Supplementary information is available on the Nature Genetics website.

ACKNOWLEDGMENTS

We thank the affected individuals and their families for participation in this study. We also thank J. Wahlström for providing samples from one of the families, P. De Camilli (Yale University) for providing the BIN1-iso8 and BIN1-BAR* cDNA constructs, P. McPherson (McGill University) for providing the BIN1 SH3 domain cDNA construct, M. Argentini for peptide mass fingerprinting, G. Duval for generation of antibodies, S. Vicaire for DNA sequencing, C. Thibault for DNA microarray analysis and H. Rohde, N. Dondaine and E. Klein for experimental help. This work was supported by the Institut National de la Santé et de la Recherche Médicale, the Centre National de la Recherche Scientifique, the Collège de France, the Agence Nationale de la Recherche and the Association Française Contre les Myopathies (AFM). A.-S.N. is the recipient of an ATER from Collège de France, and A.T. is the recipient of a fellowship from AFM.

AUTHOR CONTRIBUTIONS

Experiments were performed by A.-S.N., A.T., V.T., C.K., J.-M.G., V.B., A.O. and J.L. A.-S.N., A.T. and J.L. analyzed the data. C.W.-P., E.I. and H.K. contributed clinical samples and patient data. The study was designed and coordinated by J.-L.M. and J.L., and the paper was written by J.L.

COMPETING INTERESTS STATEMENT

The authors declare no competing financial interests.

Published online at http://www.nature.com/naturegenetics/
Reprints and permissions information is available online at http://npg.nature.com/reprintsandpermissions

1. Laporte, J. *et al.* A gene mutated in X-linked myotubular myopathy defines a new putative tyrosine phosphatase family conserved in yeast. *Nat. Genet.* **13**, 175–182 (1996).
2. Bitoun, M. *et al.* Mutations in dynamin 2 cause dominant centronuclear myopathy. *Nat. Genet.* **37**, 1207–1209 (2005).
3. Jeannet, P.Y. *et al.* Clinical and histologic findings in autosomal centronuclear myopathy. *Neurology* **62**, 1484–1490 (2004).
4. Pierson, C.R., Tomczak, K., Agrawal, P., Moghadaszadeh, B. & Beggs, A.H. X-linked myotubular and centronuclear myopathies. *J. Neuropathol. Exp. Neurol.* **64**, 555–564 (2005).
5. Wallgren-Pettersson, C. *et al.* The myotubular myopathies: differential diagnosis of the X linked recessive, autosomal dominant, and autosomal recessive forms and present state of DNA studies. *J. Med. Genet.* **32**, 673–679 (1995).
6. Dang, H., Li, Z., Skolnik, E.Y. & Fares, H. Disease-related myotubularins function in endocytic traffic in *Caenorhabditis elegans*. *Mol. Biol. Cell* **15**, 189–196 (2004).
7. Laporte, J., Bedez, F., Bolino, A. & Mandel, J.-L. Myotubularins, a large disease-associated family of cooperating catalytically active and inactive phosphoinositides phosphatases. *Hum. Mol. Genet.* **12**, R285–R292 (2003).
8. Praefcke, G.J. & McMahon, H.T. The dynamin superfamily: universal membrane tubulation and fission molecules? *Nat. Rev. Mol. Cell Biol.* **5**, 133–147 (2004).
9. Tosch, V. *et al.* A novel PtdIns3P and PtdIns(3,5)P2 phosphatase with an inactivating variant in centronuclear myopathy. *Hum. Mol. Genet.* **15**, 3098–3106 (2006).
10. Kojima, C. *et al.* Regulation of Bin1 SH3 domain binding by phosphoinositides. *EMBO J.* **23**, 4413–4422 (2004).
11. Lee, E. *et al.* Amphiphysin 2 (Bin1) and T-tubule biogenesis in muscle. *Science* **297**, 1193–1196 (2002).
12. Mandel, J.-L., Laporte, J., Buj-Bello, A., Sewry, C. & Wallgren-Pettersson, C. Developmental disorders: X-linked myotubular myopathy. in *Structural and Molecular Basis of Skeletal Muscle Diseases* (ed. Karpati, G.) 124–129 (ISN Neuropath Press, Basel, Switzerland, 2002).
13. Razzaq, A. *et al.* Amphiphysin is necessary for organization of the excitation-contraction coupling machinery of muscles, but not for synaptic vesicle endocytosis in *Drosophila*. *Genes Dev.* **15**, 2967–2979 (2001).
14. Butler, M.H. *et al.* Amphiphysin II (SH3P9; BIN1), a member of the amphiphysin/Rvs family, is concentrated in the cortical cytomatrix of axon initial segments and nodes of ranvier in brain and around T tubules in skeletal muscle. *J. Cell Biol.* **137**, 1355–1367 (1997).
15. Ramjaun, A.R., Micheva, K.D., Bouchelet, I. & McPherson, P.S. Identification and characterization of a nerve terminal-enriched amphiphysin isoform. *J. Biol. Chem.* **272**, 16700–16706 (1997).
16. Wechsler-Reya, R., Sakamuro, D., Zhang, J., Duhadaway, J. & Prendergast, G.C. Structural analysis of the human BIN1 gene. Evidence for tissue-specific transcriptional regulation and alternate RNA splicing. *J. Biol. Chem.* **272**, 31453–31458 (1997).
17. Itoh, T. & De Camilli, P. BAR, F-BAR (EFC) and ENTH/ANTH domains in the regulation of membrane-cytosol interfaces and membrane curvature. *Biochim. Biophys. Acta* **1761**, 897–912 (2006).
18. Peter, B.J. *et al.* BAR domains as sensors of membrane curvature: the amphiphysin BAR structure. *Science* **303**, 495–499 (2004).
19. Ren, G., Vajjhala, P., Lee, J.S., Winsor, B. & Munn, A.L. The BAR domain proteins: molding membranes in fission, fusion, and phagy. *Microbiol. Mol. Biol. Rev.* **70**, 37–120 (2006).
20. Sakamuro, D., Elliott, K.J., Wechsler-Reya, R. & Prendergast, G.C. BIN1 is a novel MYC-interacting protein with features of a tumor suppressor. *Nat. Genet.* **14**, 69–77 (1996).
21. Owen, D.J. *et al.* Crystal structure of the amphiphysin-2 SH3 domain and its role in the prevention of dynamin ring formation. *EMBO J.* **17**, 5273–5285 (1998).
22. Ge, K. *et al.* Mechanism for elimination of a tumor suppressor: aberrant splicing of a brain-specific exon causes loss of function of Bin1 in melanoma. *Proc. Natl. Acad. Sci. USA* **96**, 9689–9694 (1999).
23. Ge, K. *et al.* Losses of the tumor suppressor BIN1 in breast carcinoma are frequent and reflect deficits in programmed cell death capacity. *Int. J. Cancer* **85**, 376–383 (2000).
24. Korshunov, A., Sycheva, R. & Golanov, A. Recurrent cytogenetic aberrations in central neurocytomas and their biological relevance. *Acta Neuropathol. (Berl)* (2006).
25. Muller, A.J. *et al.* Targeted disruption of the murine Bin1/Amphiphysin II gene does not disable endocytosis but results in embryonic cardiomyopathy with aberrant myofibril formation. *Mol. Cell. Biol.* **23**, 4295–4306 (2003).
26. Wechsler-Reya, R.J., Elliott, K.J. & Prendergast, G.C. A role for the putative tumor suppressor Bin1 in muscle cell differentiation. *Mol. Cell. Biol.* **18**, 566–575 (1998).
27. Engel, A.G. & Franzini-Armstrong, C. *Myology, Basic and Clinical* (McGraw-Hill New York, 2004).
28. Buj-Bello, A. *et al.* The lipid phosphatase myotubularin is essential for skeletal muscle maintenance but not for myogenesis in mice. *Proc. Natl. Acad. Sci. USA* **99**, 15060–15065 (2002).
29. Thompson, J.D., Gibson, T.J., Plewniak, F., Jeanmougin, F. & Higgins, D.G. The CLUSTAL_X windows interface: flexible strategies for multiple sequence alignment aided by quality analysis tools. *Nucleic Acids Res.* **25**, 4876–4882 (1997).
30. Green, S., Issemann, I. & Sheer, E. A versatile in vivo and in vitro eukaryotic expression vector for protein engineering. *Nucleic Acids Res.* **16**, 369 (1988).

Supplementary Figure 1 SNP haplotype analysis of 4 unrelated consanguineous CNM patients for the 2q14 region containing the *BIN1* gene. Patients AAT68, ADR71 and LF41 have mutations in *BIN1*, while we did not find nucleotide variant in ABJ25 by sequencing all exons and intron-exon boundaries. A and B denote the 2 alleles of each SNP: AA and BB, homozygous alleles, AB, heterozygous. Homozygous regions were considered significant from 25 consecutive homozygous SNPs.

SNPs	Chromosomal regions	AAT68	ADR71	LF41	ABJ25
rs725139	2 q13		AB		
rs724496	2 q13	AB	AA		
rs1374161	2 q13	BB	…		
…	… …	…	…		
rs951431	2 q14.1	AA	AA	AA	AB
rs959031	2 q14.1	BB	BB	AB	BB
rs332704	2 q14.2	BB	BB	AA	BB
rs1534100	2 q14.2	BB	AA	AB	BB
rs874816	2 q14.2	AA	BB	AB	AA
rs959111	2 q14.2	BB	BB	AA	BB
rs2311398	2 q14.2	AA	AA	AA	AA
rs724691	2 q14.3	BB	AA	BB	AA
rs724692	2 q14.3	AA	AA	AA	BB
rs1368107	2 q14.3	AA	AA	AA	BB
rs723839	2 q14.3	BB	BB	BB	AA
rs1371494	2 q14.3	BB	BB	AB	BB
rs1607327	2 q14.3	BB	AA	AB	BB
rs294665	2 q14.3	AA	AA	AA	AA
rs167164	2 q14.3	AA	AA	AA	AA
rs951528	2 q14.3	BB	BB	BB	BB
rs2203772	2 q14.3	AA	AA	AA	AA
rs2419559	2 q14.3	AA	BB	AA	BB
rs1980356	2 q14.3	AA	AA	AB	AA
rs1405090	2 q14.3	AA	AA	AB	AA
rs1589908	2 q14.3	BB	BB	AB	BB
rs1343822	2 q14.3	BB	BB	AA	BB
rs2090030	2 q14.3	AA	BB	BB	AA
rs779991	2 q14.3	AA	AA	AA	BB
rs1186396	2 q14.3	AA	AA	AA	BB
rs1170578	2 q14.3	BB	BB	BB	AA
rs1367244	2 q14.3	AA	AA	BB	AA
rs2421084	2 q14.3	AA	BB	AA	AA
rs717601	2 q14.3	BB	BB	AB	BB
rs1583471	2 q14.3	BB	BB	BB	BB
rs763829	2 q14.3	BB	BB	BB	BB
rs1820556	2 q14.3	AA	BB	AA	BB
rs2404175	2 q14.3	AA	AA	AA	AA
rs1370229	2 q14.3	BB	AA	BB	BB
rs1316775	2 q14.3	BB	BB	BB	AA
rs1404073	2 q21.1	AA	AA	AA	AA
rs1097703	2 q21.1	BB	BB	BB	BB
rs1349734	2 q21.1	AA	AA	BB	AA
rs1946798	2 q21.2	AA	AA	AB	AA
rs2320399	2 q21.2	BB	BB	AB	BB
rs2321201	2 q21.2	AA	AA	AB	AA
rs3886664	2 q21.2	BB	BB	BB	BB
rs1867898	2 q21.2	BB	BB	AA	BB
rs1564935	2 q21.2	AB	AA	BB	AA
…	… …		…		…
rs1357157	2 q22.1		…		BB
rs1395010	2 q22.1		…		AB
…	… …		…		
rs1384662	2 q22.1		AA		
rs2217964	2 q22.1		AB		

← ***BIN1***

Mutations in amphiphysin 2 (BIN1) disrupt interaction with dynamin 2 and cause autosomal recessive centronuclear myopathy

Anne-Sophie Nicot, Anne Toussaint, Valérie Tosch, Christine Kretz, Carina Wallgren-Pettersson, Erik Iwarsson, Helen Kingston, Jean-Marie Garnier, Valérie Biancalana, Anders Oldfors, Jean-Louis Mandel, Jocelyn Laporte.

Supplementary information :

Supplementary Note

Human patients were recruited based on their family history, which indicated autosomal recessive inheritance, and their clinical phenotype, which was based on clinical examination and analysis of muscle biopsies taken by the Paediatric Neurologist as part of their routine clinical evaluation. The patients presented with an early onset neuromuscular disorder and muscle biopsy showed features consistent with centronuclear myopathy with numerous fibers with central nuclei. Muscle biopsy for histology and blood samples for DNA analysis were obtained with informed consent from the patients, or from the parents, on behalf of themselves and their children (minors). Approvals to perform research on congenital myopathies, including genetic analyses, have been granted from local ethic committees (Regional Ethical Review Board in Gothenburg, North Manchester Research Ethics Committee).

Experiments on mice were performed in the animal house of IGBMC (Illkirch, France). The IGBMC complies with National laws and European Directives governing Animal housing and welfare, dissection and experimentation. The animal facility is approved by the French Ministry of Agriculture and Fisheries' veterinary services. Animal experimentation is carried out under the general supervision of licensee, Prof. Jean-Louis Mandel. Prior to dissection, mice were anesthetized by i.p. injection of ketamine followed by cervical dislocation.

Supplementary Figure 1 SNP haplotype analysis of 4 unrelated consanguineous CNM patients for the 2q14 region containing the *BIN1* gene.

Supplementary Table 1 Primers for mutation screening.

Supplementary Table 2 Polymorphisms detected in the human *BIN1* gene.

Supplementary Table 3 Clinical and genetic data of the affected individuals of the three CNM families.

Supplementary Table 1 Primers for mutation screening (sequences from 5' to 3')

Exons	Wechsler-Reya et al. J. Biol. Chem. 1997		Forward	Reverse
1	1		GTCAGTTGGCTCCGCTGT	AGGATAGGGGGACAGGTG
2	2		TGGTGACTGAGCACTCTTGG	CTCCACAAATTCAGCTCGTG
3 and 4	3 and 4		GAGAGCAGCCTGGTTCATTC	CAGAGAGGCTTGTCCCAGAG
5	5		ACATTTGCCCCCATCTTACA	GTCCTAGGCCCTGTCCTCTC
6	6		GATCCACTGGACCTGGAGTC	CACAAGGGCCTCTCACTCAC
7	6a	alternative	CCTAATTCTCTCGGCCTCAA	AGCAGAGCTCTCCCAGCA
8	7		ATGGGTGTCCACATCCAGTT	CACTCAGGCTGGACACTGC
9	8		CTGGTTTGTGCCTCTGATGA	CCTCCCACGACTCTGACTCT
10	9		ATGGGGAAAGAGGAGCTTGT	ACCAACAGGGTCACAGGAAG
11	10	alternative	TCCTCTGAGCAGAAGGGTTG	CACTGCACACAGAGCCAGAT
12	11		TGCACACACCTCTTCACACA	ATGGAGGACAACAGCAAAGC
13	12a	alternative	TGTGACTAACCGTGGCTTTG	TGGCTCTTGAGACAGAAGCA
14	12b	alternative	GTGTATGTGCGCTTGCTCTG	AGGTGATGAGGGCTGAAGG
15	12c	alternative	TGAAGCTCCCTGAGAGGTGT	CTGTGAACAGGCTAGGAGCA
16	12d	alternative	CCGCTGGTGACATTTTCTCT	CTGTCCTCACCCTCACATCC
17	13	alternative	GTTTCCTGTGTCCTGGCTGT	TCCAGCTTCCTCAACAGGAG
18	14		CTCCTGTTGAGGAAGCTGGA	AGTAGCGCCTGCACAACTTT
19	15		GCATCTGAGCCCCATACTGT	GCCAGGATGCCTGTGGTC
20	16		CCTGGAGGAGGTGTTCTCAA	GGGGTCTCCTCTTGATTTCC

Supplementary Table 2 Polymorphisms detected in the human *BIN1* gene

Position	Nucleotide change	Frequency (%)
exon1	c.1-27C>T	7,6
exon4	c.318+70C>T	2,0
exon5	c.319-19C>A	1,6
exon6	c.412-25T>C	19,7
exon6	c.487T>C	27,9
exon7	c.520-110G>A	1,8
exon8	c.699+10A>G	36,6
exon8	c.699+56C>T	8,0
exon8	c.699+57G>A	8,0
exon9	c.716C>T	6,3
exon10	c.775-4A>A	10,7
exon12	c.856-12C>A	18,3
exon12	c.893G>A	10,0
exon12	c.856+51C>T	5,0
exon12	c.956C>T	13,6
exon13	c.1004-61C>T	8,0
exon13	c.1004-41G>A	4,0
exon13	c.1004-15G>A	2,0
exon14	c.1134-92C>G	6,5
exon14	c.1239+50A>C	1,9
exon15	c.1240-21C>T	3,8
exon18	c.1400-94C>T	1,8
exon18	c.1400-44C>T	33,6
exon19	c.1573-72C>T	21,2
exon19	c.1573-63C>T	14,4
exon19	c.1573-29G>C	5,1
exon19	c.1573-18G>C	4,2
exon20	c.1675-88G>A	1,0

Exonic polymorphisms do not change the aminoacid.

Nucleotide numbering from the A of the ATG start codon in *BIN1-iso1* reference sequence (NM_139343).

Supplementary Table 3 Clinical and genetic data from affected individuals of the three CNM families.

Patients (1)	Sex	Mutation	Aminoacid change	Origin	Onset	Age (yrs)	Central nuclei	Pregnancy	Ventilation	Muscle weakness (2)	Facial weakness	Ptosis	Ophtalmoplegia	Ophtalmoparesis	Other phenotypes	Cognitive development	Cardiac function	Tumors
Family 1 AAT68	male	c.105G>T	K35N	India	birth	12	++	reduced fetal movements, oligohydramnios, IUGR (3)	normal	proximal, slowly progressive	no	yes	yes	no	contractures at birth	normal	normal	no
ACC82	female	c.105G>T	K35N		birth	died at 1yr	+	reduced fetal movements, oligohydramnios, IUGR (3)	normal	proximal	no	no	no		contractures at birth	hypodevelopment of both frontal lobes	die from viral myocarditis	no (post mortem)
ADS5	female	no DNA available			birth	died at 18hrs		reduced fetal movements, oligohydramnios, IUGR (3), premature	lung hypoplasia, ventilated from birth, die from respiratory failure	no spontaneous movement					severe joint contractures at birth		prenatal heart enlarged on scan, postnatal echocardiogram normal	
Family 2 ADR71	male	c.451G>A	D151N	Iraq	8yrs	35	++	normal	normal	proximal		no	no	no	no	normal	normal	no
Family 3 LF41	male	c.1723A>T	K575X	Iraq	birth	14	++	normal	normal	proximal, slowly progressive	yes	yes	no	yes	no	normal	normal	no

(1) All parents have first cousin consanguinity and all sequenced patients are homozygous for the mutation.
(2) Muscle weakness appears mostly proximal, but not restricted.
(3) IUGR = Intra-Uterine Growth Retardation.